Radiosonde Pressure Sensor Performance: Evaluation Using Tracking Radars

C. L. PARSONS

NASA Goddard Space Flight Center, Wallops Flight Facility, Wallops Island, VA 23337

G. A. NORCROSS AND R. L. BROOKS

GeoScience Research Corporation, Salisbury, MD 21801

(Manuscript received 9 December 1983, in final form 27 August 1984)

ABSTRACT

The pressure sensors on balloon-borne sondes relate the sonde measurements to height above the earth's surface through the hypsometric equation. It is crucial that sondes used to explore the vertical structure of the atmosphere do not contribute significant height errors to their measurements of atmospheric constituent concentrations and properties. To describe quantitatively the magnitude of the error introduced by the pressure sensor, a series of radiosonde flights was conducted at Wallops Island, Virginia. In most cases, each flight consisted of two sondes attached to a single balloon; each flight was tracked by a highly accurate C-band radar. For the first 19 radiosondes, the *standard* aneroid cell–baroswitch assembly used by the National Weather Service was the pressure sensor. The last 26 radiosondes were equipped with a *premium* grade aneroid cell–baroswitch assembly sensor and with a hypsometer. Analysis has revealed that both aneroid cell–baroswitch sensors become increasingly inaccurate with altitude. At 35 km altitude, the standard deviation of the sonde sensor–radar differences was found to be 1.838 and 0.742 km, respectively, for the standard and premium sensors. On the other hand, the hypsometer–radar differences are not strongly dependent upon altitude, and the standard deviation of the differences at 34 km was found to be 0.276 km.

1. Introduction

The standard balloon-borne radiosonde used for synoptic meteorology produces vertical profiles of temperature, pressure and humidity as a function of elapsed time. These parameters are used in the hypsometric equation to calculate the geopotential altitude at each sampling point during the balloon's flight, and most applications involving the radiosonde require geopotential height information. For example, the Electrochemical Concentration Cell (ECC) Ozonesonde uses the radiosonde's transmitter to telemeter ozone concentration data to the ground along with its ambient environmental measurements to calculate ozone mixing ratio as a function of pressure or altitude. Regardless of whether it is pressure or altitude that is required for a particular application, it is imperative that the vertical location information be accurate. Based on the data from a single radiosonde, the misplacement of a sensor's measured data point in the vertical cannot be distinguished from an error in the sensor's measurement itself. Hence, the pressure, temperature and humidity measurements of the radiosonde must be as accurate as possible. The relative importance of these measurements can be judged from the hypsometric equation

$$Z_2 = Z_1 - \frac{R_d}{g}\int_{p_1}^{p_2} \frac{T_v}{p}\,dp, \qquad (1)$$

where Z_1 and Z_2 are the geopotential heights at the bottom and top, respectively, of an atmospheric layer bounded by pressures p_1 and p_2; R_d is the gas constant for dry air, g the gravitational acceleration, T_v the virtual temperature in an incremental layer of pressure thickness dp and p the pressure. We define T_v as

$$T_v = (1 + 0.608w)T,$$

where w is the mixing ratio for water vapor. Inasmuch as the standard radiosonde is designed mainly for synoptic meteorology purposes, its vertical operating range is bounded at the top by the 10 mb or perhaps even the 30 mb standard pressure level. For the ECC ozonesonde, the region of the atmosphere between the tropopause and the balloon burst altitude is of supreme importance. Hence, this study was initiated to evaluate the altitude determination accuracy of the standard radiosonde throughout the entire balloon profile (see Appendix). The tests also included two other commercially available pressure sensors to see if they could provide improved accuracy in the stratosphere.

2. Description of the pressure sensors

The synoptic radiosonde uses an aneroid cell–baroswitch assembly as its pressure sensor. After undergoing appropriate tests to "age" the materials

in the cell until an equilibrium is reached, the cells are calibrated in the laboratory. The calibration record is then included with the hardware when sold by the manufacturer. During the testing and calibration procedures, it is possible for the manufacturer to select those units that exhibit the most stability and, hence, which are most accurately calibrated; these are hereafter referred to as the *premium* baroswitch sensors (L. Potts, VIZ Manufacturing Co., personal communications, 1983). The remaining units are labeled as *standard* baroswitches. For this study, the standard radiosondes used were VIZ Model No. 1220-410 units and the premium systems were VIZ Model No. 1207-311 units. All used telemetry frequencies of 403 MHz.

The third type of sensor involved in this study is the hypsometer. In contrast to the aneroid cell devices, which expand as the pressure to which they are subjected is reduced, the hypsometer is based upon the relationship between the boiling point of a liquid and the ambient pressure. Physically, a hypsometer consists of a chamber in which a liquid is maintained at its boiling point. The chamber is designed to minimize the presence of air diffusion and superheating of the liquid; in this way, the relationship between the vapor pressure (equaling the ambient pressure for a boiling liquid) and the liquid's temperatured is preserved. For a known liquid and by means of a calibrated thermistor that measures temperature of the liquid, the atmospheric pressure can be computed using the Clausius-Clapeyron equation. In a convenient form, this equation is given by

$$\frac{de_s}{e_s} = \frac{L_{1v}}{R_v}\frac{dT}{T^2}, \tag{2}$$

where e_s is the saturation vapor pressure of the liquid, L_{1v} the latent heat of vaporization, R_v the gas constant for the vapor phase of the liquid and T temperature in degrees Kelvin. When the thermistor is calibrated, it is found that its resistance R_T is correlated closely with temperature by an expression such as

$$\ln R_T = \frac{\beta}{T} + K, \tag{3}$$

where β and K are empirical constants. Differentiating (3) with respect to T and substituting into (2) yields

$$\frac{de_s}{e_s} = -\frac{L_{1v}}{\beta R_v}\frac{dR_T}{R_T}. \tag{4}$$

This equation describes the general relationship between the thermistor resistance and the vapor pressure, which for boiling is equal to the atmospheric pressure p. The units flown in this study were bought as auxiliary sensors within the VIZ 1207-311 radiosondes. The liquid provided was trichloro-monofluoromethane (F-11) and the thermistor calibration was included by the manufacturer as part of a total hypsometer system calibration. By rearranging (4), it is easily shown that a reduction in p results in an increase in thermistor resistance and that the altitude sensitivity increases with decreasing pressure in contrast to the aneroid cell sensors. This relationship is very promising for stratospheric applications.

3. Test procedures

a. Experiment design

To assess the accuracy of the geopotential heights computed using radiosonde measurements, it is necessary to compare these values with altitude measurements from another source. The accuracy of this "standard" must be known, and errors must be much smaller than those expected from the radiosonde data. The C-band tracking radar measurements satisfy these conditions; they were used in this study as the reference or standard data set. The radar measurements of range, azimuth and elevation were made on an aluminized retroreflector suspended a few meters beneath the sondes. When operated in such a mode, the C-band radar is capable of measuring range to within ±6 m, and elevation angle to within ±0.11° (Selser, personal communication, 1983). For worst case conditions, these range and elevation accuracy errors translate into altitude errors of 6 and 320 m, respectively. The azimuth does not affect the altitude determination. In general, the altitude measurement by these tracking radars is much superior to the larger of these numbers.

b. Launch configuration

The radiosonde flights were launched from Wallops Island during two separate campaigns. During September and October 1982, two standard radiosondes were launched on each of 10 flights (there was one sonde failure) and during December 1982–February 1983, two premium aneroid cell–baroswitch sensor/hypsometer packages were flown on each of 13 balloons. For a launch, two radiosondes were attached to a narrow platform 15.3 m beneath the balloon and were separated by 1.8 m, midpoint-to-midpoint. The radar reflector was suspended an additional 4.6 m below the sondes. This configuration is shown in Fig. 1. Each launch was tracked by radar from release to burst.

c. Data reduction

The sonde measurements of temperature, pressure and relative humidity were telemetered to standard GMD ground stations and were displayed on TMQ-5 strip-chart recorders during each balloon ascent.

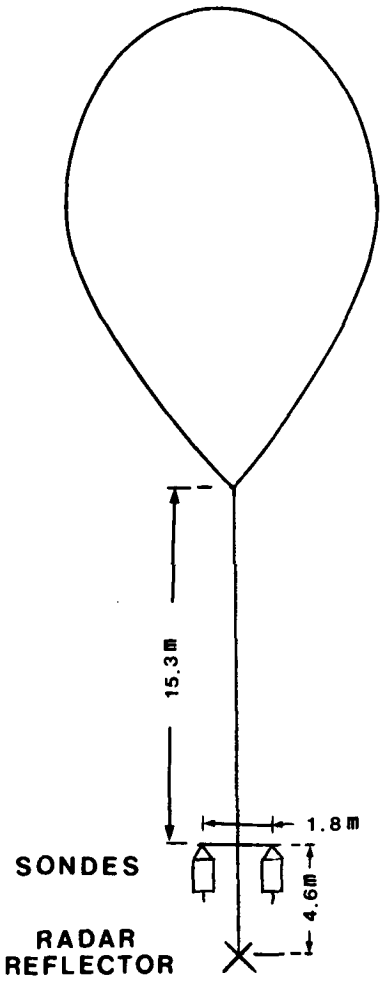

FIG. 1. Launch configuration for all sondes tested.

These outputs could be directly compared with once-per-second radar measurements by relating both to the time of launch, which was known to ±1 second. The sonde data were processed using the hypsometric equation in operational software that produced pressure-derived geopotential altitude values at a nominal rate of one per minute of flight time. The radar data, recorded at the radar site onto magnetic tape, were also processed through operational software packages that produced geometric altitude values once per second of flight time. These radar altitudes were subsequently converted to geopotential altitudes using standard techniques and 38°N latitude in the conversions. The operational programs also correct for the earth's curvature. Differences between the sonde- and radar-determined geopotential altitude values were then computed and plotted versus the radar heights. The results of this data comparison are described in the following section.

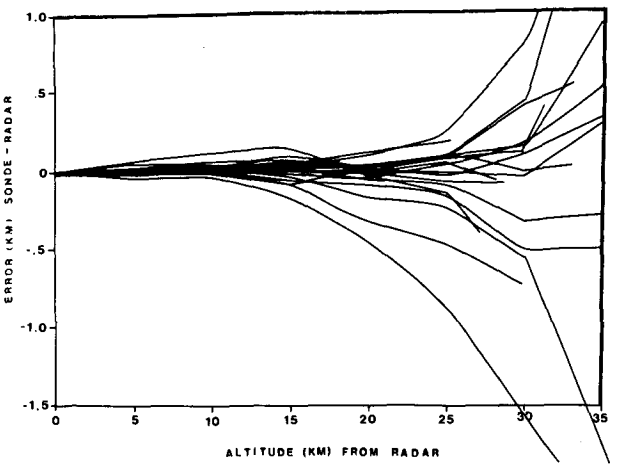

FIG. 2. Difference of sonde-derived altitude minus radar altitude for each standard baroswitch sonde.

4. Results

For the first series of flights using standard aneroid cell–baroswitch sensors, 19 sets of usable data were collected. In Fig. 2 the sonde–radar differences are plotted. The sensors generally perform well up to about 25 km; above that level, there is rapid divergence. During the second launch series, premium aneroid cell–baroswitch sensors and hypsometers were both flown on each radiosonde. A total of 26 radiosondes were released; the data are plotted in Fig. 3 for the premium cell. Details of the two launch series can be found in Norcross and Brooks (1983). The radar data used in these comparisons have not been corrected for refraction because the performance of the sondes is poor at the higher altitudes regardless of the refraction. It will be shown that the refraction

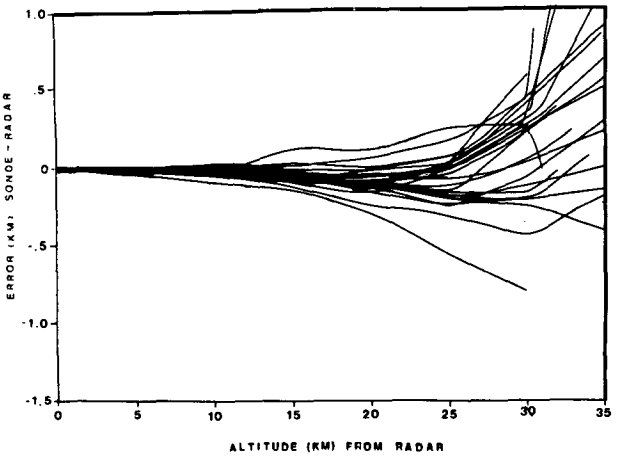

FIG. 3. As in Fig. 2 but for each premium baroswitch sonde.

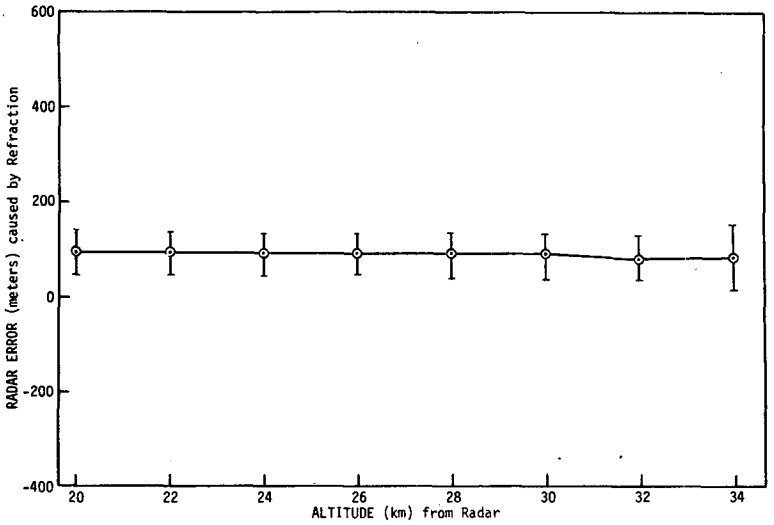

FIG. 4. Mean and one standard deviation radar altitude errors due to refraction as a function of radar altitude.

effect is small compared to the differences shown in Figs. 2 and 3.

The hypsometer data presented here are confined to the upper portion of the atmosphere. The baroswitch is wired so that for the lower altitudes, humidity data are telemetered to the ground. Beginning at switch setting number 136 (about 75 mb pressure altitude for most aneroid cell assemblies), the hypsometer data are telemetered instead. This is conveniently at the upper end of the humidity sensor's range and near the altitude at which F-11 first begins to boil. (A resistance heater submerged in the fluid is used to initiate boiling near this altitude.) When (1) is used to compute the altitude corresponding to the top of a particular pressure layer, the bottom of that layer is also needed. Hypsometer pressure readings below about 75 mb are not available. Hence, the lower altitudes must be computed using aneroid cell data. Thus, the hypsometer analyses are started at a convenient altitude around 70 mb, using the computed altitude at the pressure from the aneroid cell in the same radiosonde package.

Preliminary study of the hypsometer results indicated that sensor results agreed closely with the radar-

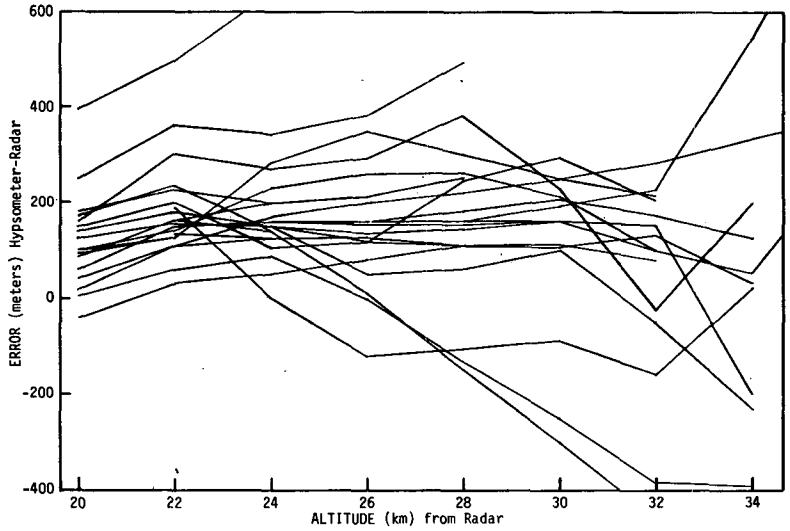

FIG. 5. Difference of hypsometer-derived altitude minus radar altitude for each hypsometer flight. The radar altitudes are corrected for refraction.

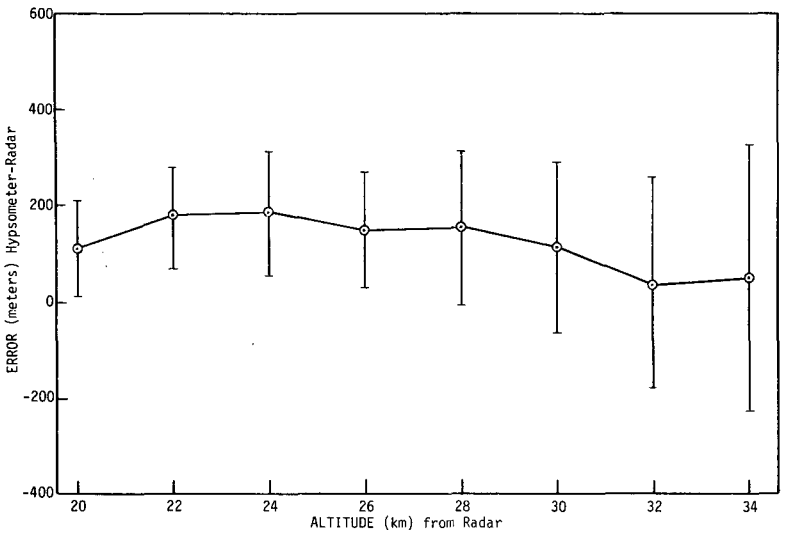

FIG. 6. Mean and one standard deviation of hypsometer-derived altitude and radar altitude differences as a function of radar altitude. The radar altitudes are corrected for refraction.

computed altitudes. Hence, the refraction correction was needed to produce the best possible comparison. The radar data were reprocessed using a refraction model based upon a mean profile for the atmospheric refraction index. The results are shown in Fig. 4. For the hypsometer releases, it is seen that the mean refraction correction above 20 km is approximately 90 m in additional altitude. The standard deviation is also fairly constant with altitude and is about 40 m in magnitude. The standard deviation is primarily determined for this data set by one flight, which was carried downwind at a very low elevation angle by strong winds. The corrected hypsometer–radar altitude differences are plotted in Fig. 5. Note that the scale is significantly larger than the scale used in Figs. 2 and 3. Figure 6 shows the mean difference and the standard deviation of the differences from Fig. 5. Even at 34 km, the mean hypsometer–radar altitude difference of 48 m is less than the worst-case inaccuracy of 320 m that may result from the radar itself!

Comparisons of the performance of the premium cells and hypsometers with the standard cells can best be made statistically. Table 1 contains the standard deviations of the baroswitch–radar differences at 5 km height intervals, and Table 2 contains the hypsometer–radar results. These same data are shown graphically in Fig. 7. Results for the standard cell agree closely with the results obtained by Schmidlin *et al.* (1982). It is obvious that the selection process does produce sondes in which aneroid cell behavior at low pressures is superior to that of the standard cell. It should also be noted that part of the premium versus standard sonde differences may be due to improvements in thermistor performance as well. Literature from the VIZ Manufacturing Company

TABLE 1. Sonde minus radar standard deviations.

	Standard baroswitch		Premium* baroswitch	
Altitude (km)	Number of observations	1σ (m)	Number of observations	1σ (m)
35	4	1838	19	742
30	14	605	22	322
25	19	258	24	167
20	19	139	24	134
15	19	91	24	118
10	19	48	24	56
5	19	30	24	32

* Two anomalous baroswitch sondes were edited prior to this computation.

TABLE 2. Hypsometer minus radar standard deviations.

	Hypsometer	
Altitude (km)	Number of observations	1σ (m)
34	10	276.4
32	15	219.4
30	16	174.8
28	19	162.3
26	19	121.5
24	21	128.6
22	21	102.4
20	18	99.4

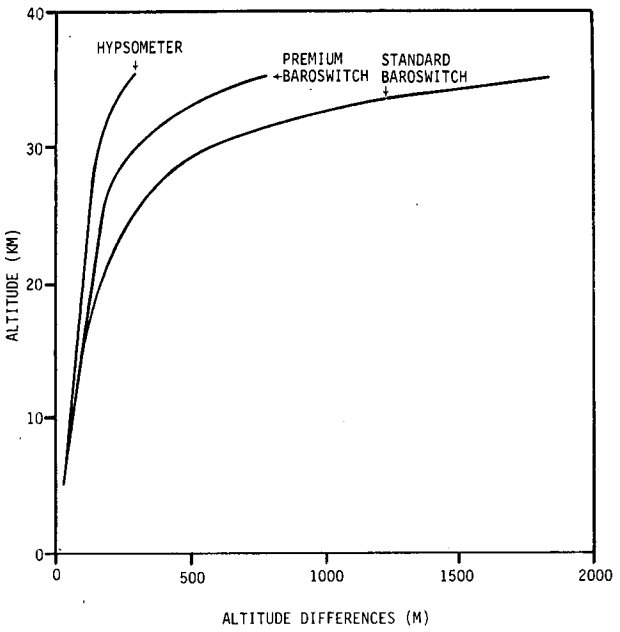

FIG. 7. The rms differences between the sonde-derived altitudes and radar altitudes for each sonde type tested.

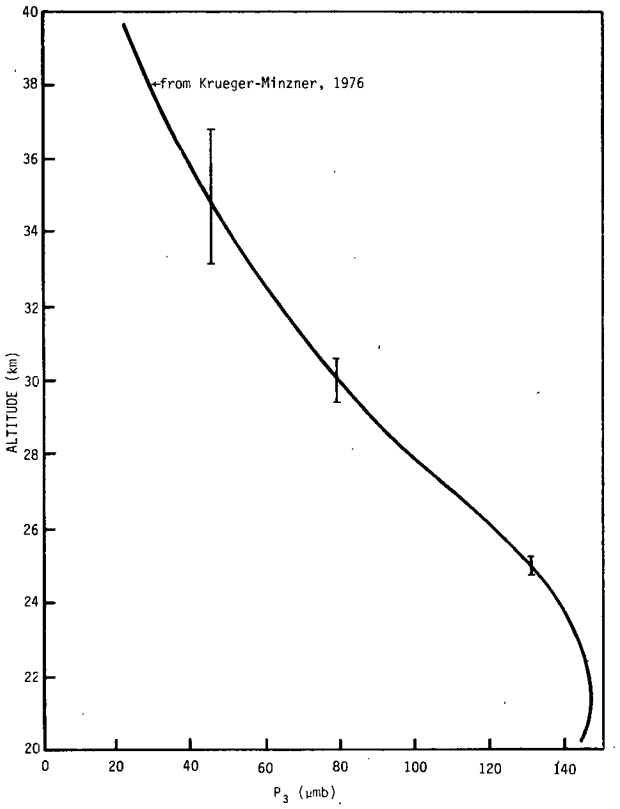

FIG. 8. Ozone profile vertical misplacement errors (± one standard deviation) for the standard baroswitch sonde using the 1976 Krueger-Minzner ozone model.

cites an rms temperature error of 0.4°C for the standard sonde and 0.1°C for the premium package. It is also obvious that in the stratosphere, the hypsometer is clearly the preferred pressure sensor. With its standard deviation of 276 m at 34 km, it agrees with the radar heights to within the error bounds of radar measurement. It should be noted that the hypsometer used in these tests, which was manufactured by VIZ Manufacturing Company, has a small reservoir. On two flights the hypsometer record was terminated prematurely prior to balloon burst. It is suspected that in those cases, the hypsometer vials ran out of fluid.

The impact of these results on the ozonesonde's performance is examined in Figure 8. The Krueger-Minzner midlatitude ozone profile (U.S. Standard Atmosphere, 1976) is plotted and at 25, 30 and 35 km, the altitude uncertainty for the standard baroswitch assembly is shown (± one standard deviation). By translating the ozone profile up and down by these uncertainties, it is seen that at 35 km, the misplacement of the profile results in ozone partial pressure errors of 11.5 and 9.0 μmb, respectively. In terms of percentage error, these are 123.47 and 78.51% and are clearly unacceptable. At 30 km these percentage errors are 108.12 and 94.54%, and at 25 km they are 101.15 and 98.55%. Since the uncertainties for the hypsometer sensor are smaller than these latter results, the hypsometer-equipped sonde should have pressure-sensor related errors of less than 3 μmb throughout the 0–34 km range of the balloons used in this study. Obviously, for the ozonesonde application, the hypsometer is required to achieve the acceptable accuracy in the stratosphere.

5. Summary

The pressure-measuring performance of standard baroswitches, premium baroswitches and hypsometers in balloon-borne sondes has been correlated with tracking radars.

The standard and premium baroswitches generally perform well up to about 25 km altitude, above which they introduce rapidly divergent altitude errors. For measurements above 25 km, hypsometers provide significantly more reliable pressure measurements.

Acknowledgments. The authors appreciate the cooperation and assistance provided by members of the Joule and Computer Science Corporation on-site support groups. Also, Al Holland and Arnold Torres of NASA contributed valuable technical guidance and Harry Bloxom and Dempsey Bruton of NASA provided operational support. Finally, we would like to thank one of the reviewers for his thorough and diligent analysis of our paper.

APPENDIX

Derivation of Height Error Formulas due to Temperature and Pressure Errors

From (1) the hypsometer equation for a single layer in the atmosphere can be written as

$$Z_2 = Z_1 - \frac{R_d}{g}\left(\frac{T_{v_1} + T_{v_2}}{2}\right)\ln\left(\frac{P_2}{P_1}\right). \quad \text{(A1)}$$

Within this layer, a height error δZ_2 is introduced if there is an error δT_2 in the temperature measurement at the top of the layer. Then,

$$Z_2 + \delta Z_2 = Z_1 - \frac{R_d}{g}\left[\bar{T}_v + \frac{\delta T_2}{2}\right]\ln\left(\frac{P_2}{P_1}\right), \quad \text{(A2)}$$

$$\delta Z_2|_T = \frac{-R_d}{g}\left(\frac{\delta T_2}{2}\right)\ln\left(\frac{P_2}{P_1}\right). \quad \text{(A3)}$$

If the temperature is measured properly, but there is an error in the pressure measurement P_2, then the resulting height error can be found from the formula derived as follows. From (A1),

$$\frac{P_2}{P_1} = \exp\left[\frac{g}{R_d}(Z_1 - Z_2)\left(\frac{2}{T_{v_1} + T_{v_2}}\right)\right]. \quad \text{(A4)}$$

For an error δP_2,

$$\frac{P_2}{P_1} + \frac{\delta P_2}{P_1} = \exp\left[\frac{2gZ_1}{R_d(T_{v_1} + T_{v_2})}\right]\exp\left[\frac{-2g(Z_2 + \delta Z_2)}{R_d(T_{v_1} + T_{v_2})}\right]. \quad \text{(A5)}$$

Solving for δZ_2,

$$\exp\left[\frac{-2g\delta Z_2}{R_d(T_{v_1} + T_{v_2})}\right] = \left(\frac{P_2}{P_1} + \frac{\delta P_2}{P_1}\right)\frac{P_1}{P_2} = 1 + \frac{\delta P_2}{P_2}, \quad \text{(A6)}$$

$$\delta Z_2|_P = \frac{-R_d}{g}T_v \ln\left(1 + \frac{\delta P_2}{P_2}\right). \quad \text{(A7)}$$

For altitudes more than one layer thickness above the surface, Eq. (A1) must be implemented iteratively. This can be written mathematically as

$$Z_n = Z_0 - \frac{R_d}{g}\sum_{i=1}^{N}\left(\frac{T_{v_{i-1}} + T_{v_i}}{2}\right)\ln\frac{P_i}{P_{i-1}}, \quad \text{(A8)}$$

where Z_n is the altitude at the level of interest and Z_0 is the altitude at the earth's surface.

To evaluate the effect of various temperature and pressure errors on computed values of Z_n, the 1976 Standard Atmosphere was used to model the accurately measured temperature and pressure profiles. Then systematic temperature and pressure errors were introduced to produce the following results.

Error description	Resulting height error (m) at 32 km
1% increase in pressure	−84
1 mb increase in pressure	−705
1% increase in temperature	+320
1 K increase in temperature	+140

REFERENCES

Norcross, G. A., and R. L. Brooks, 1983: Balloon-borne pressure sensor performance evaluation utilizing tracking radars. NASA CR 168345, 57 pp.

Schmidlin, F. J., J. Olivero and S. Nestler, 1982: Can standard radiosonde system meet special atmospheric research needs? *Geophys. Res. Lett.*, **9**, 1109–1112.

U.S. Standard Atmosphere, 1976: NOAA-S/T 76-1562, U.S. Govt. Printing Office, Washington, DC, 227 pp.